Journal of University of Science and Technology Beijing
Vol.8(2001), No.2, p.91

Metallurgy

Behavior of Non-metallic Inclusions in Centrifugal Induction Electroslag Castings

Xichun Chen, Jie Fu, Deguang Zhou, Weiguo Xu

Metallurgy School, University of Science and Technology Beijing, Beijing 100083, China
(Received 2000-09-20)

Abstract: In order to know the behavior of non-metallic inclusions in centrifugal induction electroslag castings (CIESC), non-metallic inclusions in 5CrMnMo and 4Cr5MoSiV1 were qualitatively and quantitatively analyzed. The largest size of inclusions in the casting and the thermodynamic possibility of TiN precipitation in steel were also calculated. The results show that sulfide inclusions are evenly distributed and the content is low. The amount of oxide inclusions in CIESC 4Cr5MoSiV1 steel is close to the ESR steel and lower than that in the EAF steel, and there are some differences along radial direction. Nitride inclusions are fine and the diameter of the largest one is 3–4 μm. With the increase of the centrifugal machine's rotational speed, the ratio of round inclusions increases and the ratio of sharp inclusions decreases. According to the experiment and the calculation results, it is pointed out that the largest diameter of non-metallic inclusions in the CIESC 4Cr5MoSiV1 casting is only 6.6 μm, and [N%][Ti%] in 4Cr5MoSiV1 steel should be controlled less than 4.4×10^{-5} in order to further reduce the amount and size of TiN inclusions.

Key words: centrifugal induction electroslag casting; non-metallic inclusions; 4Cr5MoSiV1 steel; 5CrMnMo steel; TiN precipitation

Centrifugal induction electroslag casting (CIESC) is a new electroslag metallurgy technology to cast shaped and hollow castings developed by the University of Science and Technology Beijing in the early of 1990's, which combined the virtues of electroslag induction melting and centrifugal casting [1]. The mechanical and service properties of the CIESC products can meet the requirements specified to the corresponding forgings, and it is proved by practice that its products such as GCr15V cold extruding wheel, 4Cr5MoSiV1 assel roller and slanting roller, 5CrMnMo hot compaction roller had 150%–300% as long working life as the same type of forgings. The cost of the CIESC products is lower than that of the CESC ones as no need of the consumable electrodes [2, 3].

The material properties depend on its structure, and the non-metallic inclusions in the castings have very important influence on its mechanical and service properties. Therefore, the behavior of the non-metallic inclusions in CIESC castings was studied in this article.

1 Experimental

(1) Sampling method.

9 pieces of samples were obtained from three different altitudinal levels(top-1#, middle-2#, and bottom-3#) and for each level, three were taken from radial direction (outer-1, middle-2, inner-3) of the 5CrMnMo hot compaction roller and 4Cr5MoSiV1 (AISI H13) assel roller blanks produced by CIESC, as shown in **figure 1**, and their chemical compositions are listed in **table 1**.

(2) Comparison study.

The inclusion content comparative studies for CIESC, ESR and EAF melting steels (H13) were carried out.

(3) Analytical method.

Metallographic microscope and image analysis sys-

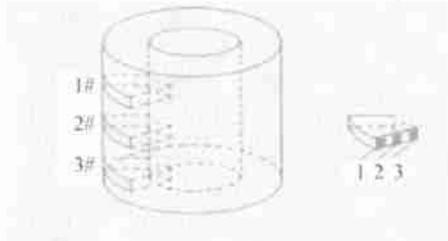

Figure 1 Sampling position.

Table 1 Chemical Composition of the specimens produced by CIESC (mass fraction) %

Grade	C	Si	Mn	P	S	Cr	Mo	V	H	O	N	Ti	Al
5CrMnMo	0.53	0.22	1.42	0.16	0.006	0.75	0.21	—	—	—	—	—	—
4Cr5MoSiV1	0.44	0.93	0.33	0.015	0.005	4.93	1.20	1.08	0.000 47	0.03 5	0.015	0.005 7	0.030

tem were used to determine the type, size, quantity and distribution of non-metallic inclusions, and scanning electron microscope (SEM) was used to determine the composition of non-metallic inclusions.

2 Results

The non-metallic inclusions in specimens (5CrMnMo) are oxide, sulphide and nitride inclusions mainly, which are shown in **figure 2** respectively.

The qualitatively and quantitatively analysed results (see **table 2**) show that sulphide inclusions are evenly distributed and their content is low, while the content of oxide inclusions is high. There are some differences along radial direction caused by centrifugal force. From the outer section to the inner section, the content and size of inclusions increase.

The comparison study results show that the amount of oxide inclusions in CIESC samples (4Cr5MoSiV1) is close to that of 4Cr5MoSiV1 produced by ESR and lower than that of 4Cr5MoSiV1 produced by EAF melting process. Moreover, the all oxide inclusions in CIESC steel are finer than 8 μm and a majority of which are finer than 2 μm. The composition of oxide inclusions is mainly Al_2O_3 and SiO_2, which exist almost spherically in castings. The amount of sulphide inclusions in sample is low due to its low [S] content. At the same time, the single or compound nitride inclusions are fine and most of them are smaller than 1 μm. When all the nine samples were observed with SEM, the largest nitride inclusions is only 3–4 μm in more than 270 field ranges.

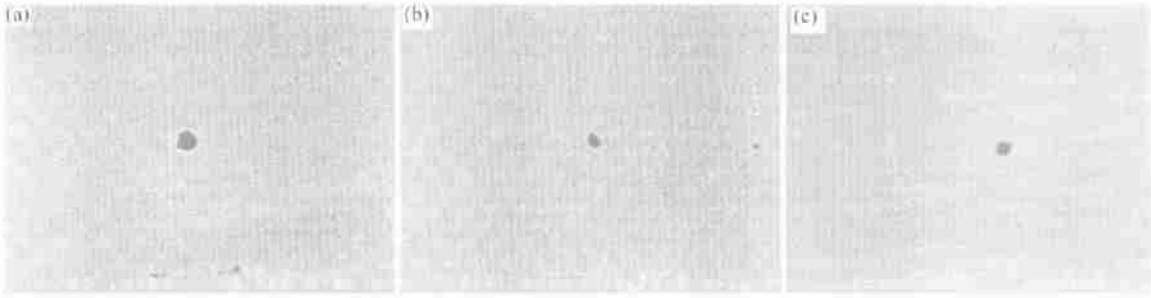

Figure 2 Oxide, sulphide and nitride inclusions in specimens (5CrMnMo), (a) oxide inclusion; (b) sulphide inclusion; (c) nitride inclusion.

Table 2 Size and distribution of oxide inclusions and sulphide inclusions in specimens (5CrMnMo)

Type	No.	Area fraction / %	Numbers of non-metallic inclusions per mm²						
			≤ 1.0 μm	1.0–2.0 μm	2.0–3.0 μm	3.0–4.0 μm	4.0–5.0 μm	5.0–6.0 μm	≥6.0 μm
Oxide inclusion	1	0.07	124	62	48	5	2	0	0
	2	0.13	75	45	36	24	9	2	0
	3	0.18	34	25	34	23	16	7	3
Sulphide inclusion	1	0.01	1	1	1	0	0	0	0
	2	0.01	2	1	1	0	0	0	0
	3	0.01	2	1	1	0	0	0	0

3 Discussion

3.1 Rotational speed

The rotational speed of mold is a very important factor, which causes the segregation of non-metallic inclusions in radial direction. At a certain rotational speed, the centrifugal force leads the inclusions "inner floating". The larger inclusions were inner floated by bigger force. Therefore, the large inclusions were gathering in the inner part of castings. With the increasing of the rotational speed, more and more inclusions are removed out of the casings.

At different rotational speeds, the ratio of sharp oxide inclusions to spherical ones (R) changed, as shown in **figure 3**. R decreased with the increase of the rotational speed (ω), which is possibly caused by different

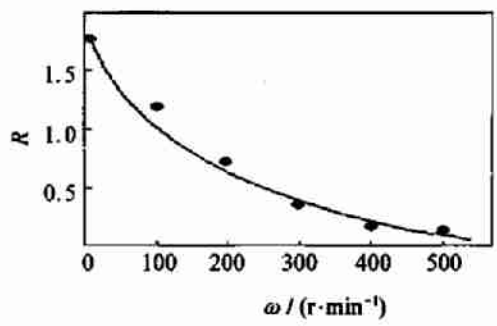

Figure 3 Effect of rotational speed on the ratio of sharp oxide inclusions to spherical ones (R).

flow velocity between inclusions and liquid steel due to the different rotational speed.

3.2 The largest size of non-metallic inclusions

The Reynolds number of non-metallic inclusions inner floating action caused by centrifugal force is:

$$Re=\frac{du}{v} \tag{1}$$

Where d is the diameter of non-metallic inclusions, supposed as 10 μm; u is the separate speed of inclusions, measured by model experiment as 0.306 cm/s; v is the kinematic viscosity, $v=0.008\ cm^2/s$. Then,

$$Re=\frac{10\times10^{-4}\times0.306}{0.008}=3.8\times10^{-2} \tag{2}$$

When $Re<1$, the inner floating speed caused by centrifugal force is [4]:

$$u=\frac{2}{9}\cdot k\cdot\frac{\rho_m-\rho_s}{\mu_m}\cdot r^2 \tag{3}$$

Under the centrifugal force affection, $k=\omega^2\cdot R'$, ω is the rotational velocity of mould; R' is the rotational radius. It is obvious that non-metallic inclusions will be removed out of the castings if its radius is larger than a critical value. The critical value can be calculated out from the following equation:

$$r_c=\left(\frac{9u_{max}\cdot\mu_m}{2k\cdot(r_m-r_s)}\right)^{1/2} \tag{4}$$

Where $R'=20$ cm, $u=0.306$ cm/s, $\mu_m=0.057\,6$ g/(cm·s), $\omega=900$ r/min $=94.2$ rad/s, $\rho_m=7.2\ g/cm^3$, $\rho_s=2.86\ g/cm^3$. At last, it can be obtained that

$r_c=3.3$ μm.

So, the largest diameter of the non-metallic inclusions is 6.6 μm in the experimental condition, and it is consistent with the experimental results.

3.3 Thermodynamic calculation of TiN precipitation

The precipitation condition of TiN inclusions in 4Cr5MoSiV1 can be calculated with thermodynamic method:

$$Ti_{(s)}=Ti_{(l)},\quad \triangle G_1^{\ominus}=15\,500-8.0\,T \tag{5}$$

$$Ti_{(l)}=[Ti],\quad \triangle G_2^{\ominus}=-69\,500-27.28\,T \tag{6}$$

$$1/2N_{2(g)}=[N],\quad \triangle G_3^{\ominus}=10\,500+20.37\,T \tag{7}$$

$$Ti_{(s)}+1/2N_{2(g)}=TiN_{(s)},\quad \triangle G_4^{\ominus}=334\,500+93.0\,T \tag{8}$$

$$[Ti]+[N]=TiN_{(s)},$$

$$\triangle G^{\ominus}=\triangle G_4^{\ominus}-\triangle G_3^{\ominus}-\triangle G_2^{\ominus}-\triangle G_1^{\ominus} \tag{9}$$

$$\triangle G^{\ominus}=-29\,100+107.91\,T \tag{10}$$

The equilibrium constant K is decided by the following equation:

$$K=\frac{\alpha_{TiN_{(s)}}}{\alpha_{[Ti]}\alpha_{[N]}}=\frac{1}{f_{Ti}[\%Ti]f_N[\%N]} \tag{11}$$

$$\lg K=-\frac{\triangle G^{\ominus}}{2.3RT}=\frac{15\,220}{T}-5.64 \tag{12}$$

$$-\frac{15\,220}{T}+5.64=\lg[\%Ti]+\lg[\%N]+\lg f_{Ti}+\lg f_N \tag{13}$$

Where

$$\lg f_{Ti}=\left(\frac{2\,557}{T}-0.365\right)\lg f_{Ti(1\,873\,K)},$$

$$\lg f_{Ni}=\left(\frac{3\,280}{T}-0.75\right)\lg f_{N(1\,873\,K)}\ [5].$$

At 1 873 K, the activity coefficient in liquid steel can be calculated:

$$\lg f_{i(1\,873\,K)}=\Sigma(e_i^j[\%j])\ (j=C,\ Si,\ Mn,\ \cdots;\ i=Ti,\ N.) \tag{14}$$

The interaction coefficients in liquid steel at 1 873 K are listed in **table 3**.

Table 3 The interaction coefficients e_i^j in liquid steel at 1873K (j = C, Si, Mn, ···)

i	C	Si	Mn	P	S	H	O	N	Al	Cr	Ti	Mo	V
Ti	−0.165	0.05	0.004 3	−0.064	−0.11	−1.1	−1.8	−1.8	0.12	0.055	0.013	−0.011	−0.093
N	0.13	−0.047	−0.21	0.045	0.007	0.002	0.005	0.0	0.028	−0.047	−0.537	—	—

$$\lg f_{Ti(1\,873\,K)}=e_{Ti}^{C}[C]+e_{Ti}^{Si}[Si]+e_{Ti}^{Mn}[Mn]+e_{Ti}^{P}[P]+e_{Ti}^{S}[S]+e_{Ti}^{H}[H]+e_{Ti}^{O}[O]+e_{Ti}^{N}[N]+e_{Ti}^{Al}[Al]+e_{Ti}^{Cr}[Cr]+e_{Ti}^{Ti}[Ti]+e_{Ti}^{Mo}[Mo]+e_{Ti}^{V}[V],$$

$$\lg f_{N(1\,873\,K)}=e_{N}^{C}[C]+e_{N}^{Si}[Si]+e_{N}^{Mn}[Mn]+e_{N}^{P}[P]+e_{N}^{S}[S]+e_{N}^{H}[H]+e_{N}^{O}[O]+e_{N}^{N}[N]+e_{N}^{Al}[Al]+e_{N}^{Cr}[Cr]+e_{N}^{Ti}[Ti]+e_{N}^{Mo}[Mo]+e_{N}^{V}[V].$$

At last, the thermodynamic condition of TiN inclusion precipitation during solidification can be expressed as:

$$\lg[\%N][\%Ti]=-\frac{14\,734}{T}+5.51 \tag{15}$$

From the above equation, it can be calculated that TiN will precipitate in liquid steel at 1 768 K (liquidus temperature) when [N%][Ti%] is equal to 1.5×10^{-3} in the experimental 4Cr5MoSiV1 steel. With the temperature falling down, TiN will precipitate from austenite in the solid-liquid zone according to references [6] and [7]. It is formulated as the following equation:

$$\lg[\%N][\%Ti]=-\frac{13\,850}{T}+4.01 \tag{16}$$

Figure 4 is drawn based on equations (15) (around liquidus temperature 1 768 K) and (16) (around solidus

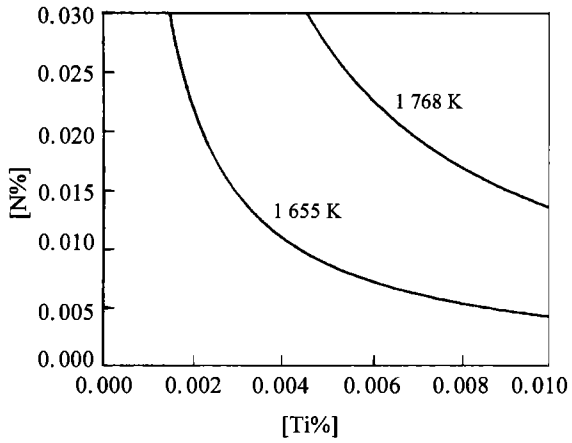

Figure 4 Stability diagram of TiN precipitation in 4Cr5MoSiV1 steel.

temperature 1 655 K) to desribe the possibility of TiN precipitation. From figure 4 it can be seen that in the experimental condition ([Ti%]=0.0057, [N%]=0.015), TiN will precipitate above the solidus temperature (1 665 K), and the precipitated TiN will be gathering and growing with rather sufficient time and temperature condition. Therefore, [N%] [Ti%] in 4Cr5MoSiV1 steel should be controlled less than 4.4×10^{-5} in order to insure no TiN precipitation over solidus temperature.

4 Conclusions

(1) The results show that sulphide inclusions are evenly distributed and the content is low, while the content of oxide inclusions is high and there are some differences along axial direction in the samples (5CrMnMo); and in the sapmles (4Cr5MoSiV1), the amount of oxide inclusions is close to that of 4Cr5MoSiV1 produced by ESR and lowers than that of 4Cr5MoSiV1 produced by EAF melting process.

(2) With the increase of the centrifugal machine's rotational speed, the ratio of round inclusions increases and the ratio of sharp inclusions decreases.

(3) The largest diameter of non-metallic inclusions in samples is only 6.6 μm.

(4) Nitride inclusions are fine and the diameter of the largest one is 3–4 μm, and [N%][Ti%] in 4Cr5MoSiV1 steel should be controlled less than 4.4×10^{-5} in order to further reduce the amount and size of TiN inclusions.

References

[1] J. Fu, W. Xu, Y. Wang, et al.: *A Method of Producing Shaped Hollow Castings Using Centrifugal Induction Electroslag Casting*, National Invention Patent, No.91105455.3, 1998.

[2] W. Xu, X. Chen, J. Fu, et al.: *Journal of University of Science and Technology Beijing*, 20(1998), p. 431.

[3] J. Fu, Z. Miao, W. Xu, et al.: [In:] *Proceedings of 11th ICVM*, Antibes-Juan-les Pins, France, 1992, p. 174.

[4] X. Zhang: *Metallurgy Transfer Principle*. Beijing: Metallurgical Industry Press, China, 1987, p. 164.

[5] В. А.Григорян: *Physicochemical Calculation of Steel Making Process*. Beijing: Metallurgical Industry Press, China, 1993, p. 102.

[6] W. Liu, J. J. Jonas: *Metal Trans. A*, 20A (1989), No.8, p. 1361.

[7] W. Liu, S. Yue, J. J. Jonas: *Metal Trans. A*, 20A (1989), No. 10, p. 1907.